ORGANIC CHEMISTRY FRONTIERS

RESEARCH ARTICLE

View Article Online
View Journal | View Issue

Cite this: *Org. Chem. Front.*, 2019, **6**, 2266

Orthogonally arranged tripyrrin–BODIPY conjugates with an "edge to plane" mode†

Chun-Liang Hou,‡[a] Yuhang Yao,‡[b] Da Wang,[a] Jing Zhang*[a] and Jun-Long Zhang *[b]

Received 28th March 2019,
Accepted 23rd April 2019

DOI: 10.1039/c9qo00445a

rsc.li/frontiers-organic

We designed new molecular conjugates, consisting of two strong fluorophores, tripyrrin and BODIPY moieties. Crystal structures demonstrated that the BODIPY is nearly perpendicular to the tripyrrin plane, directly linked in an orthogonal geometry, in a new "edge to plane" mode with covalently bonded chromophore peripheries. Furthermore, substitutions on BODIPY can modulate the photophysical properties, which can be explained by energy transfer *via* a FRET mechanism. This not only enriches the repertoire of multichromophoric system but also expands the scope of tripyrrin for constructing molecular functional materials.

Introduction

Tripyrrins are a type of linear oligopyrrole, which can be found as biopyrrin and biotripyrrins *a*, *b* during the biodegradation of hemin and chlorophylls.[1] Thanks to the rich chemistry of oligopyrroles, great progress has been made particularly in the synthesis of various π-expanded porphyrins as important building blocks.[2] Moreover, the intriguing electronic structures, coordination ability and photophysical properties render tripyrrins attractive molecules in organic optoelectronics and biological studies, encouraged by the success of their cousins boron dipyrromethane (BODIPYs)[3] and porphyrinoid.[4] However, the flexibility of linear tripyrrins results in non-radiative decay, which makes achieving a high luminescence challenging.[5] To circumvent this, bridging the terminal pyrroles with benzene-1,4-diol affords rigid tripyrrins, which enhances the fluorescence remarkably.[6] Importantly, the bridged phenyl group was found to be perpendicular to the tripyrrin plane and capable of imparting intermolecular interactions and thus solid state emission.[6] Therefore, this orthogonal structure stimulates us to explore tripyrrins as acceptor or donor units in multichromophoric systems.[7]

The relative orientation of a donor and acceptor pair in multichromophoric systems plays a critical role in the energy/electron transfer process at a given donor–acceptor separation.[8] The orthogonal orientation between a donor and acceptor pair[7,9] has long been considered to result in weak coupling, which facilitates energy/electron transfer either through space or through bond mechanisms.[10] Thus, constructing an orthogonal structure between a donor–acceptor pair has been attracting increased attention for potential applications in solar cells, OLEDs, bio-imaging and sensing.[9b–d,11] According to the orientation and link between donor and acceptor, we tentatively divided into "edge to edge" and "edge to plane" modes (Scheme 1). The common mode is "edge to edge" (Scheme 1a), which directly connects the peripheries of porphyrinoids, BODIPYs, perylenes and spirobifluorenes, extensively employed as models for energy/electron transfer.[12] Another mode is "edge to plane" (Scheme 1b) which usually links the different moieties by coordination bonds through the axial position of metalloporphyrinoids or phthalocyanines.[13]

In this work, we chose BODIPY (4,4-difluoro-4-bora-3a,4a-diazas-indacene, BDP) dye as a moiety, which is well-known for tunable absorption/emission *via* β-substitution of BODIPY,[3a] to construct tripyrrin–BODIPY conjugates. Systematic modifications of BODIPY can be made allowing for

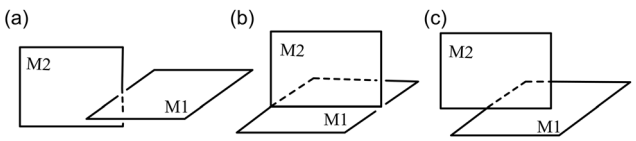

Scheme 1 Orthogonal molecular conjugates in (a) "edge to edge" mode; (b) "edge to plane" mode (axial); (c) "edge to plane" mode (peripheral). (M1 or M2 represents the different moiety).

[a]*Center of Materials Science and Optoelectronics Engineering, College of Materials Science and Opto-Electronic Technology, University of Chinese Academy of Sciences, Beijing 100049, P. R. China. E-mail: zhangj271@ucas.ac.cn*
[b]*Beijing National Laboratory for Molecular Sciences, State Key Laboratory of Rare Earth Materials Chemistry and Applications, College of Chemistry and Molecular Engineering, Peking University, Beijing 100871, P.R. China. E-mail: zhangjunlong@pku.edu.cn*

†Electronic supplementary information (ESI) available. CCDC 1889398–1889400 and 1896685. For ESI and crystallographic data in CIF or other electronic format see DOI: 10.1039/c9qo00445a

‡These authors contributed equally to this work.

a comprehensive analysis of the structure–property relationship of such molecular conjugates. Importantly, we reported new orthogonal molecular conjugates with "edge to plane" mode (Scheme 1c), consisting of covalently linking two strong fluorophores: tripyrrin and BODIPY, which may be potentially used as a new molecular platform without axial coordination.

Results and discussion

Synthesis and characterization

Starting from pentafluorophenyltripyrrane, we synthesized 2,5-pentafluorophenyl tripyrrin dibromide by treatment with 2 equiv. of *N*-bromosuccinimide (NBS) in anhydrous CH_2Cl_2 at −78 °C for 1 h and consequent oxidation of 2,3-dichloro-5,6-dicyano-1,4-benzoquinone (DDQ) at room temperature for 10–15 minutes without isolating the mid product of pentafluorophenyltripyrrane dibromide.[6] After removing excess DDQ by flash column, the reaction between 2,5-hydroxybenzaldehyde and tripyrrane dibromide in the presence of potassium carbonate as a base in acetonitrile at 80 °C afforded the cross-link coupling product ($1^1E,1^2Z,5^1E,5^2Z$)-2,4-bis(perfluorophenyl)-$1^2H,3^1H,5^2H$-6,8-dioxa-1,3,5(2,5)-tripyrrola-7(1,4)-benzenacyclo octaphane-7^2-carbaldehyde (**1**) in a yield of 55%.

Synthesis of tripyrrin–BODIPY conjugates (**2** and **3**) was achieved according to the previous synthesis of BODIPY (Scheme 2).[14] **1** reacted with pyrrole or 2,4-dimethyl-pyrrole in the presence of a catalytic amount of trifluoroacetic acid (TFA) following DDQ oxidation. **2** or **3** was obtained by consequent reaction with boron trifluoride.[14] However, **2** is unstable in solution at room temperature,[15] thus **3** is used as a parent molecule to further peripheral modification of BODIPY. Next, the reaction between 1-iodopyrrolidine-2,5-dione (NIS) and **3** gave the 3,3′-diiodo product **4** in a yield of *ca.* 98%.[16] Sonogashira coupling of **4** and 1-ethynyl-4-methoxybenzene catalyzed by CuI and $Pd(PPh_3)_4$ afforded **5** in a yield of *ca.* 20%.[17] The corresponding BODIPY dyes of **3–5** (**BODIPY 3–5** in Scheme 2) were also synthesized as comparisons according to the literature.[18] These new compounds have been characterized by HR ESI-MS, ^1H, ^{13}C and ^{19}F NMR, FT-IR spectrometry and spectroscopy (Fig. S1–S27†) and the detailed synthetic procedure is listed in the ESI.†

X-ray crystallography

Single crystals of **1** (CCDC 1889398), **2** (CCDC 1889399), **4** (CCDC 1889400) and **5** (CCDC 1896685)† were obtained by slow diffusion of hexane to chloroform solution. **1** and **2** both crystallized in the orthorhombic space group, whereas **4** and **5** is in the monoclinic space group (Table S1, Fig. S28–S34†). As shown in Fig. 1a, the bridging benzaldehyde moiety in **1** is almost perpendicular to the tripyrrin ring (dihedral angle is 86.2°). Importantly, the crystal structures of **2** and **4** display a larger tilt of the benzene ring (Fig. 1b and c, dihedral angles

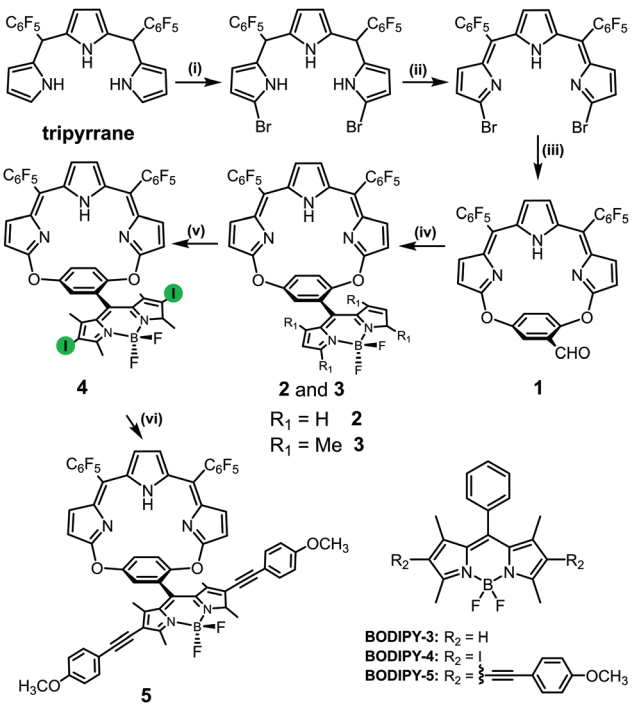

Scheme 2 Synthetic method of **1–5**. Reagents and conditions: (i) NBS, CH_2Cl_2, −78 °C, 50 min; (ii) DDQ, room temperature, 10–15 min; (iii) 2,5-hydroxybenzaldehyde, K_2CO_3, acetonitrile, reflux, 2 h; (iv) pyrrole or 2,4-dimethyl-pyrrole, TFA, NEt_3, $Et_2O{\cdot}BF_3$, CH_2Cl_2, room temperature, 2.5 h; (v) 1-ethynyl-4-methoxybenzene, NIS, CH_2Cl_2, room temperature, 30 min; (vi) CuI, $Pd(PPh_3)_4$, THF : NEt_3 = 5 : 1, 70 °C, 24 h.

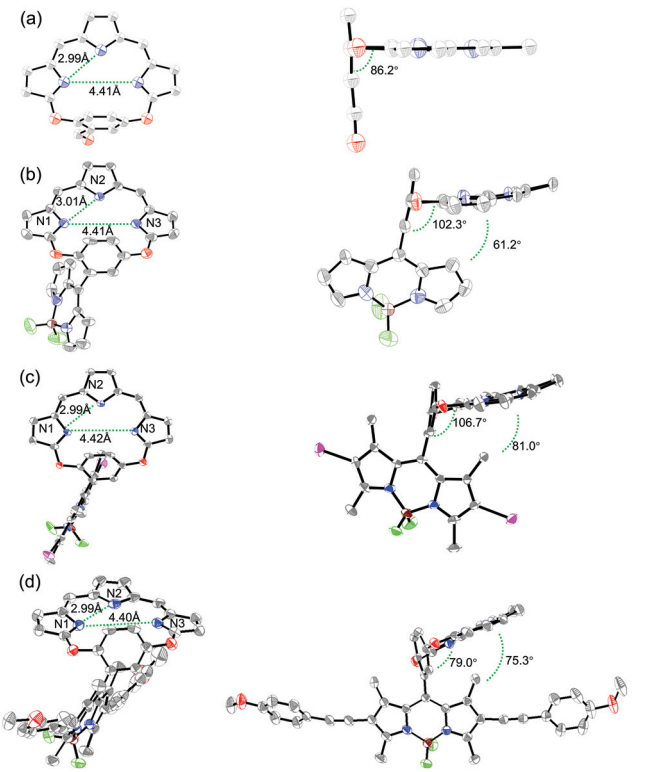

Fig. 1 X-ray crystal structures of (a) **1**, (b) **2**, (c) **4** and (d) **5**. Top view (left) and side view (right). Hydrogen atoms, *meso*-substituted moieties and solvent molecules are omitted for clarity.

are 102.3 and 106.7°, respectively), comparable to that of the previously reported *p*-benziporphyrin.[19] In **2**, the indacene plane of BODIPY is also tilted to the tripyrrin ring with a dihedral angle of 61.2°, indicating an "edge to plane" mode. **4** shows a similar structure as **2**, and the indacene plane of BODIPY is tilted to the tripyrrin plane with a dihedral angle of 81.0°. Compared with **2** and **4**, **5** showed a similar dihedral angle (79.0°) between the phenyl ring and the tripyrrin plane. Notably, the cavity of the macrocycle is considerably larger than that of the *p*-benziporphyrin. The N1–N2, N2–N3 and N1–N3 distances for **2**, **4**, **5** are 2.99–3.01 and 4.40–4.41 Å, respectively, which are not favourable for metal coordination. These results suggest clearly that the orthogonal orientation between tripyrrin and BODIPY, is different from that previously reported for porphyrinoid or BODIPY molecular dyads in the "edge to edge" mode.[6,19]

Photophysical properties

Photophysical studies for **1** and **3–5** were performed in dichloromethane as described in Table 1 and Fig. 2. Absorption of **1**, **3–4** covered the 300–600 nm region. **3** shows a sharp band centred at 512 nm with a weak absorption at 318 nm, while the maximum absorption of **4** is at 544 nm, along with a shoulder band at 508 nm. **5** displays intense bands at 318, 535 and 595 nm, accompanied by a shoulder at 500 nm. Comparison with the absorption of **1** and BODIPY-**3** suggests that the absorption of **3** can be reproduced by linear combination of those of **1** and **BODIPY-3** (Fig. 3a).[18] The absorption of **4** and **5** could also be superimposed by the absorption of **1** and the corresponding BODIPYs[18] (Fig. 3b and c) but with more red-shift of 14 and 23 nm than that of **3** (6 nm), suggesting that the substitution of the BODIPY moiety plays an important role on the electronic structure of molecular conjugates.

Upon excitation at 500 nm, as shown in Fig. 2b and S35–S46,† **3** displays weak and broad emission maximum at 595 nm (Φ < 0.1%) with bi-exponential decay lifetimes of 0.2 (93.6%) and 1.9 ns (9.7%). While **4** and **5** display strong and broad emission centered at 570 (Φ = 2.2%) and 653 nm

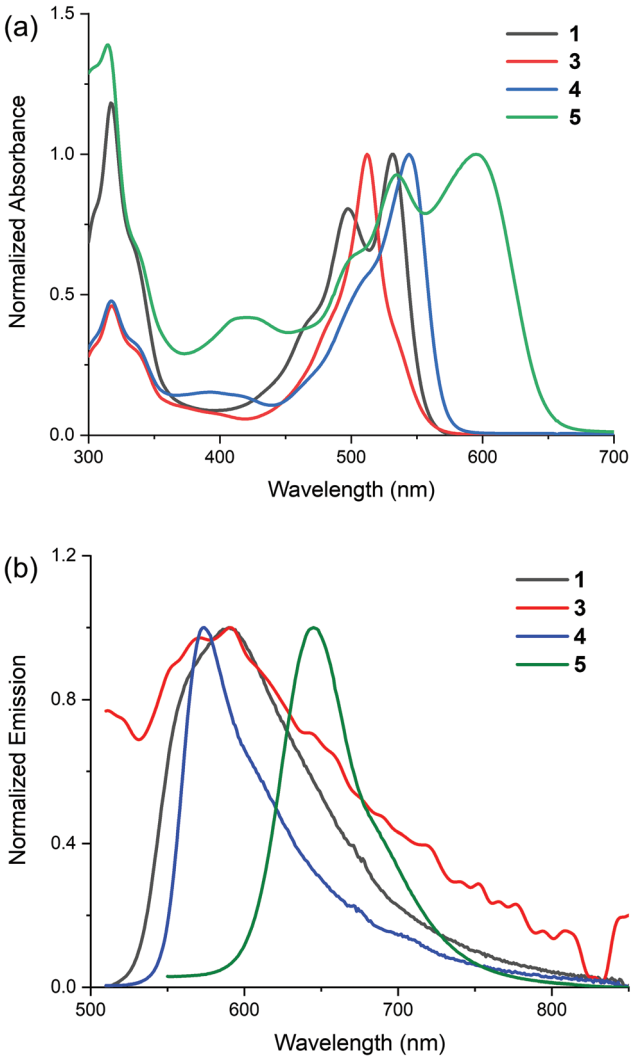

Fig. 2 (a) Absorption and (b) emission of **1** and **3–5** in CH_2Cl_2.

Table 1 Photophysical data of absorption and emission of **1** and **3–5** in CH_2Cl_2 solution at room temperature

Comp.	Absorption λ_{max}/nm (lg ε)[a]	Emission λ_{em}[a]/nm	τ[b]/ns	Φ_f[c] (%)
1	317 (4.58), 497 (4.38), 532 (4.45)	592	0.2	6.3
3	318 (4.71), 512 (5.03)	595	0.2 (90.3%), 1.9 (9.7%)	<0.1%
4	318 (4.60), 544 (4.95)	570	0.3	2.2
5	318 (4.35), 420 (3.82), 535 (4.21), 595 (4.25)	653	0.7	9.7

[a] All photophysical analyses were carried out in anhydrous CH_2Cl_2 at room temperature. [b] Lifetimes were measured on LifeSpec-II Picosecond Lifetime spectrometers. [c] Quantum yields were measured using an Edinburgh Analytical Instrument FLS-980 equipped with an integrating sphere.

(Φ = 9.7%), respectively. The lifetime decays of 0.3 and 0.7 ns were calculated and analysed using the convolution of a Gaussian function accounting for the instrumental response function (IRF) and one or two exponential functions due to the very short lifetime to avoid interference from the instrument. Comparative studies of the absorption and emission spectra of tripyrrins with the corresponding BODIPY dyes in **3**, **4** and **5** has been performed as shown in Fig. 3d–f. For **3**, the emission of BODIPY moiety is almost overlapped with the absorption of the tripyrrin unit, suggesting the BODIPY moiety can transfer energy to the tripyrrin acceptor and **3** displays a tripyrrin-type fluorescence. The low quantum yield of **3** might be ascribed to the non-radiative decay arising from the rotational flexibility of the phenyl group in the BODIPY moiety for less steric hindrance. This is supported by the significantly enhanced tripyrrin centered fluorescence (236 folds) of **3** along with decreasing temperature from 300 to 100 K (Fig. S47 and S50†), which is probably due to the suppression of intramolecular rotations at low temperature. **4** displays a complicated, broadened

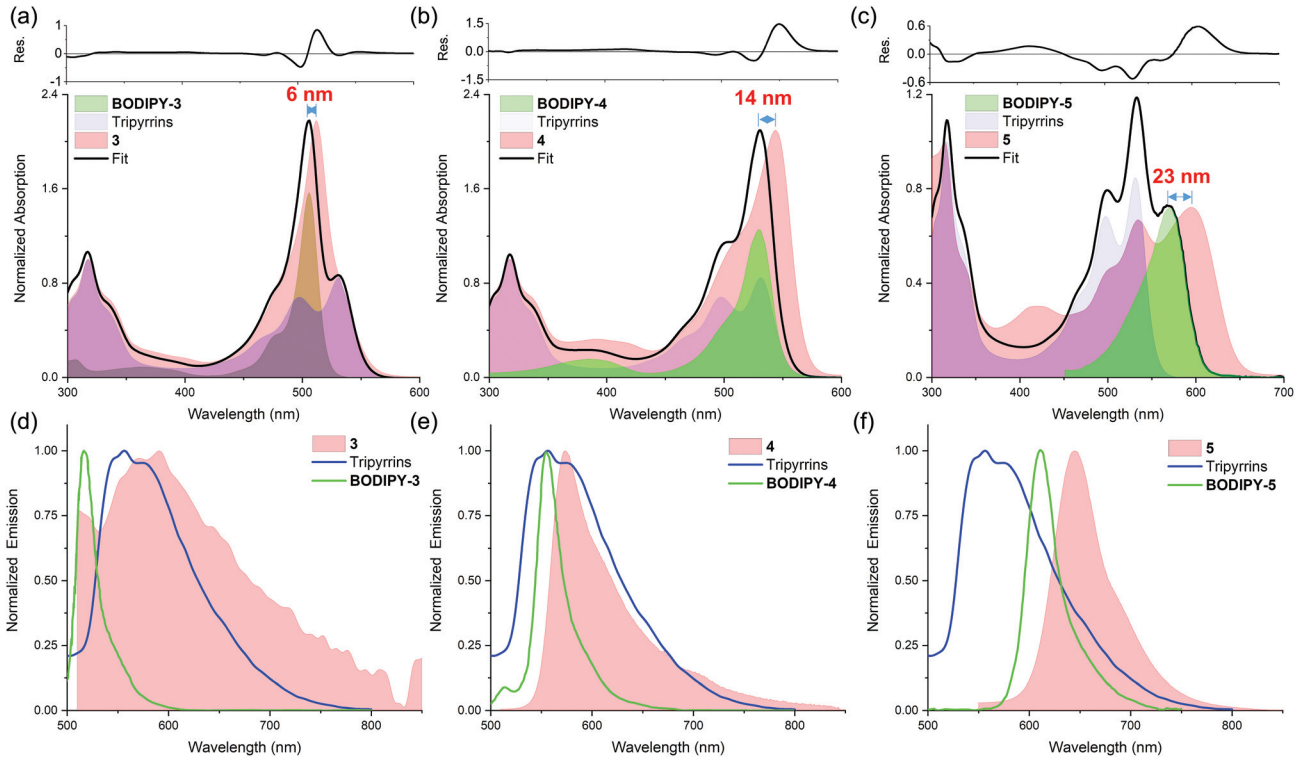

Fig. 3 Absorption spectra of (a) **3**, (b) **4** and (c) **5** reproduced by a linear combination of the spectra of corresponding BODIPY dyes[18] and tripyrrins in CH_2Cl_2, and the comparison of emission spectra between (d) **3**, (e) **4**, (f) **5** and the corresponding BODIPY dyes as well as tripyrrin dye.

emission between BODIPY and tripyrrin. This is due to similar energy levels of the BODIPY and tripyrrin moieties as shown in Fig. 3b. It is noteworthy that the heavy atom effect of iodine does not lead to phosphorescence of **4** at either room temperature even in degassed conditions (Fig. S37†) or at 100 K (Fig. S48†).[20] **5** displays the BODIPY dominated emission at either room temperature or 100 K (Fig. S49 and S51†). This could be explained by FRET (fluorescence resonance energy transfer) from the overlap of the absorption of **BODIPY-5** and the emission of tripyrrins. This is also supported by the largely diminished emission of tripyrrins as shown in Fig. 2b. In addition, **3–5** emit weak red fluorescence in the broad range of 550–850 nm in the solid state (Fig. S52†). Different from previously reported rigid tripyrrins,[6] **3–5** cannot form *J*-aggregation (Fig. S32–S34†) due to the steric hindrance of orthogonal BODIPY moieties.

To understand the electronic structures of **1**, **3–5** at ground-state, DFT and TDDFT calculations were performed at the B3LYP/6-31G(d) level.[21] The energy diagrams and the corresponding nodal patterns of the frontier molecular orbitals (FMOs) were shown in Fig. 4. The trend of HOMO–LUMO gap (H–L gap) in **3–5** follows the order of **3** > **4** > **5** consistent to the hypsochromic-shifted absorption observed in **3–5**. This demonstrates the effect of methyl substitution, iodine-substitution and extended conjugation of BODIPY unit on the H–L gap. In **3–5**, HOMO and LUMO+1 localized on BODIPY, and HOMO−1 (except **5**) and LUMO mainly localized on the tripyrrin unit, (Fig. 4b). TDDFT computational results indicated that the vertical excitations at 512, 544 and 535 nm of **3–4** are local excitation of π–π* localized in the tripyrrin moiety (HOMO−1 → LUMO, ~97%, Table S2†). And the absorption at 318 nm of **3–5** is contributed from the high energy excitation configurations localized in the tripyrrin moiety (Table S2†). In addition, the absorption at 595 nm in **5** can be assigned to the excitation of π–π* localized in the BODIPY moiety (HOMO → LUMO+1, 95%). These theoretical calculation results are in accordance with the experimental data and facilitate understanding of the energy transfer in BODIPY–tripyrrin conjugates.

Electrochemical properties

To further explore the possibility of charge separation as the additional non-radiative channel of the excited state in such molecular conjugates, we measured the cyclic voltammetry (CV) of the complexes to estimate the redox properties of ground states. As shown in Fig. S53–S59,† **3–5** showed irreversible oxidation and reduction waves. Then, differential pulse voltammetry (DPV) for **3–5** was performed to obtain the electrochemical redox potentials as listed in Table 2 and Fig. S60–S66.† The differences between electrochemical redox potentials obtained by DPV and $E_{1/2}$ of the reversible waves in CV are within 0.03 V (Table 2) for tripyrrin and BODIPY-**3** and **4**,

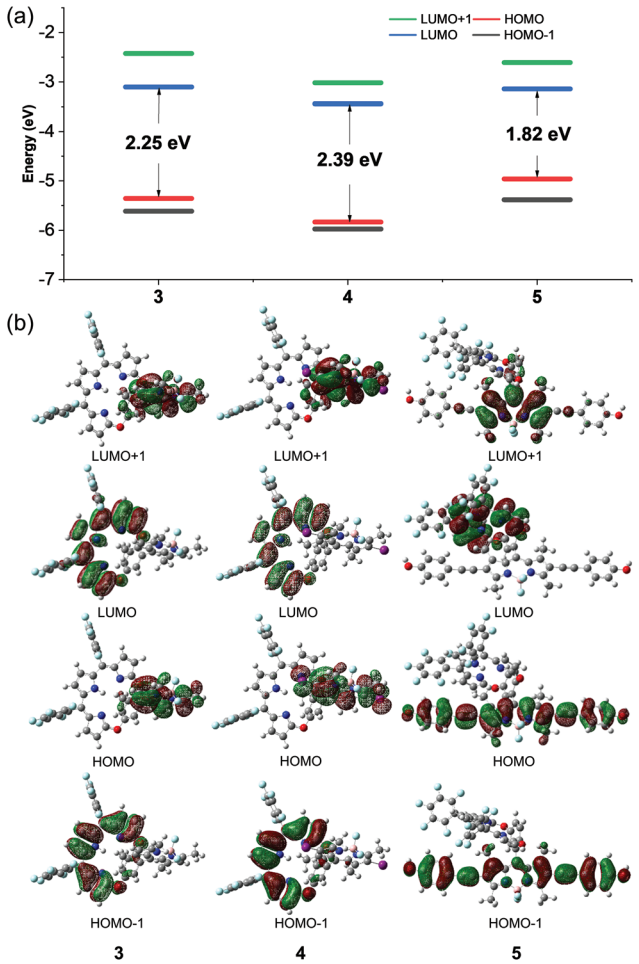

Fig. 4 (a) Energy diagram of **3–5** and (b) nodal patterns of the frontier molecular orbitals of **3–5**.

Table 2 Electrochemical redox potentials of tripyrrins, **3–5**, and the corresponding BODIPY dyes[a]

Compound	E_{OX}/V	E_{RED}/V
1	0.82(0.03[b])	−1.45(0[b]), −1.70(0[b])
3	0.75, 0.93, 1.03	−1.40, −1.61
BODIPY-3	0.75(0.01[b])	−1.73(0.02[b])
4	0.85, 0.95, 1.08	−1.35, −1.46, −1.81
BODIPY-4	0.89(0.01[b])	−1.45(0.01[b])
5	0.61, 0.90	−1.36, −1.54
BODIPY-5	0.59	−1.50(0[b])

[a] Differential pulse voltammetry (DPV) in nitrogen-saturated CH_2Cl_2 containing a 0.10 M $^tBu_4N[PF_6]$ supporting electrolyte. A Pt counter electrode, a 3 mm diameter glassy carbon working electrode, and an Ag/AgCl reference electrode were used. The potentials presented in this table are referenced to the internal standard Fc^+/Fc potential ($E_{Fc+/Fc}$ = 0.53 V). Scan rate: 100 mV s^{-1}. T = 20 °C. [b] Difference *vs.* $E_{1/2}$ of the reversible waves observed in cyclic voltammetry.

which were used to estimate the Gibbs free-energy changes (ΔG_{CS}) of photoinduced electron transfer (PET) and the charge-separated state (CSS) energy levels. The first oxidation waves of **3–5** originate from the corresponding BODIPY dyes (ΔE < 0.05 V), while other oxidation waves are likely from tripyrrins (ΔE = 0.08–0.26 V). The first reduction waves in **3–5** are from tripyrrins. This is in the line with the DFT calculated frontier molecular orbitals (FMOs).

$$\Delta G_{CS} = e[E_{ox} - E_{RED}] - E_{00} + \Delta G_S \quad (1)$$

$$\Delta G_S = \frac{e^2}{4\pi\varepsilon_0\varepsilon_S}\left(\frac{1}{2R_D} + \frac{1}{2R_A} - \frac{1}{R_{CC}}\right). \quad (2)$$

To study the possibility of intramolecular PET, the ΔG_{CS} values of **3–5** in CH_2Cl_2 were calculated using the Weller equation (eqn (1) and (2)).[22] ΔG_S is the static coulombic energy (eqn (2)), where e = electronic charge, E_{OX} is the potential for one-electron oxidation of the electron-donor unit, E_{RED} is the potential for one-electron reduction of the electron-acceptor unit, E_{00} is the energy level for the singlet excited state approximated by the fluorescence emission and absorption [(E_{abs}(max) + E_{em}(max))/2], ε_S is the static dielectric constant of the solvent (8.9 for CH_2Cl_2), R_{CC} is the center-to-center separation distance determined by density functional theory (DFT) optimization of the geometry, R_D is the radius of the electron donor, R_A is the radius of the electron acceptor, and ε_0 is the permittivity of free space (Fig. S67–S69†). The energies of the CSS (E_{CCS}) and the free-energy change of the charge recombination process (ΔG_{CR}) were calculated using eqn (3) and (4).

$$E_{CS} = e[E_{ox} - E_{RED}] + \Delta G_s \quad (3)$$

$$\Delta G_{CR} = -(\Delta G_{CS} + E_{00}). \quad (4)$$

The Gibbs free-energy changes (ΔG_{CS}) for putative electron transfer are all positive except for the electron transfer from **BODIPY-5** to tripyrrin in **5** (Table 3), indicating that the intramolecular PET in **3–4** is thermodynamically unfavourable. Even the only negative driving force of electron transfer from **BODIPY-5** to tripyrrin in **5** is also negligible (−0.093 eV). In addition, the positive values of Gibbs free-energy change of the charge recombination process (ΔG_{CR}) also suggest an unfavourable charge separation process. These results suggest that, in the tripyrrin-BODIPY **3–5**, the charge separation between donor and acceptor could not occur upon light irradiation.

Table 3 Free-energy changes of **3–5**: ΔG_{CS}, E_{CSS}, and ΔG_S in CH_2Cl_2[a]

Electron transfer	ΔG_{CS}/eV	E_{CSS}/eV	ΔG_S/eV	ΔG_{CR}/eV
Tripyrrin[b] → **BODIPY-3**[c]	0.272	2.70	0.148	−2.35
BODIPY-3[b] → tripyrrin[c]	0.095	2.35	0.148	−2.70
Tripyrrin[b] → **BODIPY-4**[c]	0.156	2.38	0.043	−2.38
BODIPY-4[b] → tripyrrin[c]	0.027	2.31	0.043	−2.31
Tripyrrin[b] → **BODIPY-5**[c]	0.294	2.29	−0.035	−2.29
BODIPY-5[b] → tripyrrin[c]	−0.093	2.01	−0.035	−2.01

[a] The arrow indicates the direction of charge transfer. [b] Electron donor. [c] Electron acceptor.

Conclusions

Taken together, we reported the design and synthesis of molecular conjugates constituted by tripyrrin with BODIPY fluorophores, which feature orthogonal structures between donor and acceptor with an "edge to plane" mode. The photophysical properties of these molecular conjugates were tuned by the substitution of BODIPY, which controls the energy transfer process from tripyrrin and BODIPY moieties. Importantly, analysis of charge separation as the additional non-radiative channel of the excited state following the Weller equation showed that the driven force for charge transfer from the excited state of either the tripyrrin or BODIPY moiety to the corresponding ground states is small, even positive. This demonstrated that, in the orthogonal tripyrrin–BODIPY conjugates, the vibration or/and rotation of the BODIPY moiety is a plausible non-radiative pathway for the excited state. Further dynamic studies for such new orthogonal structures are currently undergoing in our lab.

Experimental section

All reagents and materials were purchased from commercial suppliers and used as received unless otherwise indicated. UV-vis spectra were recorded on an Agilent 8453 UV-vis spectrometer equipped with an Agilent 89090A thermostat (±0.1 °C). ESI-MS spectra were recorded on Bruker APEX IV Fourier Transform Ion Cyclotron Resonance Mass Spectrometer using electrospray ionization. Mass spectrometric simulations were carried out using the IsoPro v3.0 package. MALDI-TOF-MS were recorded on an AB Sciex 5800 MALDI-TOF/TOF mass spectrometer. ^{1}H and ^{13}C NMR spectra were recorded on a Bruker-400 MHz instrument, ^{19}F NMR spectra were recorded on a Bruker-500 MHz instrument. ^{1}H and ^{13}C NMR spectra were referenced to tetramethylsilane as an internal standard. For the ^{19}F NMR spectra, trifluoroacetic acid (−77.5 ppm) was used as an external reference. Fluorescence spectra, lifetime and steady state spectra were recorded using FLS-920, FLS-980 and LifeSpec-II Picosecond Lifetime spectrometers. The absolute quantum yields were determined using an integrating sphere on the FLS-980 spectrometer. IR spectra were recorded on a Tensor 27 FTIR or a Spectrum Spotlight 200 FT-IR microscopic.

Synthesis of 2,5-bis((5-bromo-1*H*-pyrrol-2-yl)(perfluorophenyl)methyl)-1*H*-pyrrole

A solution of 132 mg (0.724 mmol, 2 equivalents) *N*-bromosuccinimide (NBS) in anhydrous dichloromethane (10 mL) was slowly added to a solution of 200 mg (0.362 mmol, 1 equivalent) tripyrrole in anhydrous dichloromethane (10 mL) in a two-necked flask under conditions of −78 °C with the nitrogen protection. The reaction was stirred for 50 min.

Synthesis of 2,5-bis((*Z*)-(5-bromo-2*H*-pyrrol-2-ylidene)(perfluorophenyl)methyl)-1*H*-pyrrole

After stirring for 50 min, the reaction was restored up to room temperature, then 245 mg (1.086 mmol, 3 equivalents) 2,3-dichloro-5,6-dicyanobenzoquinone (DDQ) was directly added to the two-necked flask. The solution was stirred for 10 to 15 minutes, then concentrated under reduced pressure and purified by a flash silica-gel column chromatography (eluent: petroleum ether/CH_2Cl_2, 1 : 1) to obtain the crude products.

Synthesis of 1

The previous crude products were added to a solution of 40 mg (0.290 mmol, 0.8 equivalents) 2,5-dihydroxybenzaldehyde and 120 mg (0.869 mmol, 2.4 equivalents) anhydrous potassium carbonate in anhydrous acetonitrile (20 mL). The reaction was stirred and refluxed for 12 h under a nitrogen atmosphere. Then the solution was concentrated under reduced pressure and purified by silica-gel column chromatography (eluent: petroleum ether/CH_2Cl_2, 5 : 1) to give a red solid of compound **1** (110 mg). Yield: 44.2%; ^{1}H NMR (400 MHz, methylene chloride-d_2) δ 10.45 (s, 1H), 10.23 (s, 1H), 7.86 (d, J = 2.8 Hz, 1H), 7.61 (dd, J = 8.7, 2.8 Hz, 1H), 7.46 (d, J = 8.7 Hz, 1H), 6.65 (dd, J = 8.2, 4.8 Hz, 2H), 6.60 (d, J = 4.8 Hz, 1H), 6.55 (d, J = 4.8 Hz, 1H), 5.89 (q, J = 3.2, 2.5 Hz, 2H). ^{13}C NMR (101 MHz, Chloroform-*d*) δ 187.4, 178.5, 154.4, 152.6, 146.9, 137.9, 137.7, 136.4, 135.9, 130.8, 130.6, 126.1, 123.3, 120.7, 120.2, 119.8. ^{19}F NMR (471 MHz, Chloroform-*d*) δ −138.68 (ddt, J = 257.5, 22.6, 10.4 Hz), −152.10 (dt, J = 41.8, 20.8 Hz), −159.34 to −163.60 (m). MALDI-TOF-MS *m*/*z*: Calcd for $C_{33}H_{11}F_{10}N_3NaO_3$ $[M + H]^+$ 710.0533, found 710.0544. IR (cm^{-1}): 3358, 1695, 1608, 1522, 1498, 1389, 1284, 1256, 1030, 990, 802, 761, 633. UV-vis absorption (CH_2Cl_2): λ_{max} (lg ε) = 317 (4.58), 497 (4.38), 532 (4.45).

Synthesis of 2

Pyrrole (0.504 mL, 14.55 mmol, 50 equivalents), compound **1** (100 mg, 0.291 mmol, 1 equivalents) and trifluoroacetic acid (1 μL) as catalyst were added into 20 mL anhydrous dichloromethane in a 100 mL three-necked flask. The reaction was stirred for 6 h under nitrogen protection at room temperature. Then DDQ (33 mg, 0.29 mmol, 1 equivalents) was added into the reaction solution, and the solution was stirred for 15 min at room temperature. Then, 0.72 mL triethylamine was added dropwise to the reaction under ice-cooling and stirred for 15 min. After removing the ice bath, 0.72 mL boron fluoride ethyl ether was also added dropwise and stirred for 2 h at room temperature. Finally, the reaction was quenched with 25 mL of saturated $NaHCO_3$ solution, then washed with distilled water (3 × 20 mL), and extracted with dichloromethane (3 × 20 mL). The organic phases were combined, dried over anhydrous Na_2SO_4, filtered and dried under reduced pressure to obtain the crude product. The crude product was purified by column chromatography (eluent: petroleum ether/dichloromethane = 3 : 1) to give a red solid of compound **2** (12 mg). Yield: 9.7%; ^{1}H NMR (400 MHz, Chloroform-d) δ 10.58 (s, 1H),

7.89 (s, 1H), 7.80 (s, 1H), 7.65–7.42 (m, 2H), 7.09 (s, 1H), 7.04 (s, 2H), 6.67 (s, 1H), 6.56 (d, J = 4.8 Hz, 2H), 6.40 (s, 1H), 6.21 (d, J = 8.5 Hz, 2H), 5.91 (s, 1H), 5.85 (s, 1H). ^{19}F NMR (471 MHz, Chloroform-d) δ −138.66 (dd, J = 24.0, 7.9 Hz), −139.08 (dd, J = 22.5, 8.3 Hz), −139.32 (dd, J = 24.5, 8.1 Hz), −144.29 (ddd, J = 104.8, 58.3, 29.1 Hz), −146.16 to −147.06 (m), −152.04 (dt, J = 82.3, 20.8 Hz), −160.72 (dtd, J = 29.8, 15.4, 8.0 Hz), −160.97 (td, J = 22.2, 8.5 Hz). MALDI-TOF-MS m/z: Calcd for $C_{41}H_{17}BF_{12}N_5O_2$ $[M + H]^+$ 850.1278, found 850.1276.

Synthesis of 3

2,4-Methylpyrrole (30 μL, 0.58 mmol, 2 equivalents), compound **1** (100 mg, 0.291 mmol, 1 equivalents) and trifluoroacetic acid (1 μL) as catalyst were added into 20 mL anhydrous dichloromethane in a 100 mL three-necked flask, and stirred for 6 h under nitrogen protection at room temperature. Then DDQ (33 mg, 0.29 mmol, 1 equivalents) was added into the reaction solution and stirred for 15 min at room temperature. Then 0.72 mL triethylamine was added dropwise to the reaction under ice-cooling and stirred for 15 min. After removing the ice bath, 0.72 mL boron fluoride ethyl ether was also added dropwise and stirred for 2 h at room temperature. Finally, the reaction was quenched with 25 mL of saturated $NaHCO_3$ solution, then washed with distilled water (3 × 20 mL), and extracted with dichloromethane (3 × 20 mL). The organic phases were combined, dried over anhydrous Na_2SO_4, filtered and dried under reduced pressure. The resulting crude product was purified by column chromatography (eluent: petroleum ether/dichloromethane = 3 : 1) to give a red solid of compound **3** (15 mg). Yield: 11.3%; ^{1}H NMR (400 MHz, methylene chloride-d_2) δ 10.70 (s, 1H), 7.58 (d, J = 1.5 Hz, 2H), 7.32 (d, J = 1.7 Hz, 1H), 6.63 (d, J = 4.7 Hz, 1H), 6.54 (dd, J = 6.0, 4.7 Hz, 2H), 6.41 (d, J = 4.8 Hz, 1H), 6.07 (s, 1H), 5.91 (d, J = 2.6 Hz, 3H), 2.52 (s, 3H), 2.46 (s, 3H), 2.00 (s, 3H), 1.62 (s, 3H). ^{13}C NMR (101 MHz, Chloroform-d) δ 174.6, 156.2, 155.0, 148.4, 143.2, 138.9, 136.5, 136.3, 136.0, 131.1, 122.2, 121.7 119.4, 118.4, 117.1, 116.5. ^{19}F NMR (471 MHz, Chloroform-d) δ −138.68 to −139.25 (m), −146.17 (dd, J = 65.9, 30.7 Hz), −152.12 (td, J = 20.8, 5.3 Hz), −160.84 (ddt, J = 47.2, 22.6, 8.6 Hz). MALDI-TOF-MS m/z: Calcd for $C_{45}H_{24}BF_{12}N_5NaO_2$ $[M + H]^+$ 928.1724, found 928.1720. IR (cm^{-1}): 3363, 1606, 1520, 1474, 1452, 1388, 1306, 1282, 1195, 1062, 1011, 910, 801, 759, 477. UV-vis absorption (CH_2Cl_2): λ_{max} (lg ε) = 318 (4.71), 512 (5.03).

Synthesis of 4

Compound **3** (100 mg, 0.11 mmol, 1 equivalents) and *N*-iodosuccinimide (NIS) (25 mg, 0.22 mmol, 1 equivalents) was added in anhydrous CH_2Cl_2 (30 mL). The reaction mixture was stirred at room temperature for 30 min. After addition of a saturated solution of $Na_2S_2O_3$, the aqueous layer was extracted with CH_2Cl_2 (3 times). The combined organic layer was dried over anhydrous Na_2SO_4, filtered, and concentrated under reduced pressure. The resulting crude product was subjected to silica gel column chromatography (eluent: petroleum ether/dichloromethane = 5 : 1) to afford compound **4** (125 mg) as red solids. Yield: 56%; ^{1}H NMR (400 MHz, methylene chloride-d_2) δ 10.70 (s, 1H), 7.62 (s, 2H), 7.31 (d, J = 2.1 Hz, 1H), 6.66 (d, J = 4.8 Hz, 1H), 6.55 (d, J = 4.7 Hz, 2H), 6.38 (d, J = 4.8 Hz, 1H), 5.94 (d, J = 2.4 Hz, 2H), 2.63 (s, 3H), 2.57 (s, 3H), 2.00 (s, 3H), 1.63 (s, 3H). ^{13}C NMR (101 MHz, Chloroform-d) δ 152.5, 150.4, 147.3, 146.8, 137.7, 137.5, 136.1, 135.9, 126.7, 126.6, 124.1, 120.7, 120.4, 120.1. ^{19}F NMR (471 MHz, Chloroform-d) δ −138.22 (ddd, J = 23.4, 8.8, 3.7 Hz), −138.73 (ddd, J = 23.3, 8.9, 3.7 Hz), −138.95 (ddd, J = 23.4, 8.7, 3.8 Hz), −139.22 (ddd, J = 23.5, 8.8, 3.7 Hz), −145.60 (ddt, J = 138.8, 74.8, 31.9 Hz), −152.03 (td, J = 21.0, 7.2 Hz), −160.78 (ddtd, J = 72.5, 51.3, 22.1, 8.4 Hz). MALDI-TOF-MS m/z: Calcd for $C_{45}H_{22}BF_{12}I_2N_5O_2$ $[M + H]^+$ 1156.9759, found 1156.9748. IR (cm^{-1}): 3367, 1651, 1605, 1521, 1388, 1257, 1209, 1179, 1095, 991, 911, 878, 709, 776, 589, 526. UV-vis absorption (CH_2Cl_2): λ_{max} (lg ε) = 318 (4.60), 544 (4.95).

Synthesis of 5

Compound **4** (50 mg, 0.043 mmol 1 equivalents), bis(triphenylphosphine) palladium(II) dichloride ($Pd(PPh_3)_2Cl_2$, 3 mg, 0.0043 mmol, 0.1 equivalents), copper(I) iodide (CuI 0.8 mg, 0.0043 mmol, 0.1 equivalents) and 22 μL 4-methoxyphenylacetylen (0.173 mmol, 4 equivalents) were added in degassed mixed solvent of tetrahydrofuran/triethylamine (5 : 1) (20 mL) under a stream of nitrogen. The mixture was kept stirring and refluxing for 24 h in a dark environment. Then the mixture was concentrated and purified by silica gel column chromatography (petroleum ether/CH_2Cl_2, 1 : 1) to obtain a purple solid compound **5** (5 mg). Yield: 9.9%; ^{1}H NMR (400 MHz, methylene chloride-d_2) δ 10.73 (s, 1H), 7.64–7.62 (m, 2H), 7.48–7.40 (m, 2H), 7.33 (s, 1H), 7.32–7.30 (m, 2H), 6.92–6.79 (m, 4H), 6.65 (s, 1H), 6.56 (dd, J = 10.4, 4.8 Hz, 2H), 6.42 (s, 1H), 5.92 (d, J = 2.4 Hz, 2H), 3.80 (d, J = 12.0 Hz, 6H), 2.69 (s, 3H), 2.63 (s, 3H), 2.12 (s, 3H), 1.78 (s, 3H). ^{13}C NMR (126 MHz, methylene chloride-d_2) δ 178.4, 138.1, 137.9, 136.6, 133.3, 133.3, 132.7, 130.4, 130.1, 127.0, 126.8, 125.6, 125.3, 124.9, 121.2, 121.2, 120.8, 120.6, 115.9, 114.6, 114.5, 55.9, 55.8, 54.3, 53.8. ^{19}F NMR (471 MHz, methylene chloride-d_2) δ −139.23 (dd, J = 23.8, 7.7 Hz), −139.75 to −139.91 (m), −139.99 to −140.23 (m), −146.31 (dd, J = 61.5, 30.4 Hz), −153.32 (td, J = 20.8, 8.6 Hz), −161.47 to −161.98 (m). MALDI-TOF-MS m/z: Calcd for $C_{63}H_{36}BF_{12}N_5O_4$ $[M + H]^+$ 1165.2663, found 1165.2696. IR (cm^{-1}): 3360, 3194, 2957, 2922, 2851, 1658, 1634, 1522, 1425, 11 123, 989, 617. UV-vis absorption (CH_2Cl_2): λ_{max} (lg ε) = 318 (4.35), 420 (3.82), 535 (4.21), 595 (4.25).

X-ray diffraction measurement

X-ray diffraction data were collected on Rigaku XtaLAB Pro: Kappa single system instrument equipped with a Mo Kα source. A suitable crystal was mounted on the diffractometer and cooled under a nitrogen stream as soon as practical after mounting to preclude desolvation. The CrysAlisPro program was employed for data processing. The structure was solved using SHELXT 2014 program[23] and refined against F^2 anisotropically for all non-hydrogen atoms per the full matrix least-squares protocol using the SHELXL 2016 program in an Olex2

GUI.[24] The Platon program package[25] was employed for squeeze processing.

Electrochemistry measurement

The electrochemistry experimental procedures were conducted with a standard three electrode configuration on a Shanghai Chenhua CHI660C electrochemical workstation at room temperature, 25 °C, under nitrogen. Cyclic voltammetry and differential pulse voltammetry experiments were recorded using glassy-carbon working electrode disks of 3 mm diameter (Cypress Systems EE040). The working electrode was treated between scans by means of a sequence of polishing with diamond paste (Buehler) of decreasing sizes (3 to 0.05 μm) interspersed by washings with purified H_2O. The auxiliary electrode was a platinum wire electrode and the reference electrode was an Ag/AgCl electrode. The potentials were referenced to the internal standard Fc^+/Fc potential ($E_{Fc+/Fc}$ = 0.53 V). All glassware for electrochemical experiments was oven dried overnight and allowed to cool to room temperature before use.

Calculation details

In this work, the hybrid density functional, B3LYP was employed for all calculations using the Gaussian 09 software package (version D.01).[26] The 6-31G(d) basis set was used for all atoms. Geometry optimizations of the singlet ground state (S_0) were carried out using the density functional theory without symmetry constraints. Frequency calculations were performed on the optimized structures to ensure that they represented true minimum energy structures as judged by the absence of imaginary frequency values (*i.e.* NImag = 0).

Conflicts of interest

There are no conflicts to declare.

Acknowledgements

We thank the National Scientific Foundation of China (NSFC) (21571007, 21621061, 21778002, 21861162008) and the National Key Basic Research Support Foundation of China (NKBRSFC) (2015CB856301) for financial support. And this work was supported by High-performance Computing Platform of Peking University.

Notes and references

1 (*a*) T. Yamaguchi, I. Shioji, A. Sugimoto, Y. Komoda and H. Nakajima, *J. Biochem.*, 1994, **116**, 298–303; (*b*) H. Falk, *The chemistry of linear oligopyrroles and bile pigments*, Springer Science & Business Media, 2012.

2 (*a*) H. Mori, T. Tanaka, S. Lee, J. M. Lim, D. Kim and A. Osuka, *J. Am. Chem. Soc.*, 2015, **137**, 2097–2106; (*b*) Y. Rao, T. Kim, K. H. Park, F. Peng, L. Liu, Y. Liu, B. Wen, S. Liu, S. R. Kirk and L. Wu, *Angew. Chem.*, 2016, **128**, 6454–6454.

3 (*a*) A. Loudet and K. Burgess, *Chem. Rev.*, 2007, **107**, 4891–4932; (*b*) Y. Ge and D. F. O'Shea, *Chem. Soc. Rev.*, 2016, **45**, 3846–3864; (*c*) Ha. Klfout, A. Stewart, M. Elkhalifa and H. He, *ACS Appl. Mater. Interfaces*, 2017, **9**, 39873–39889; (*d*) B. Bertrand, K. Passador, C. Goze, F. Denat, E. Bodio and M. Salmain, *Coord. Chem. Rev.*, 2018, **358**, 108–124.

4 (*a*) A. Mahmood, J. Y. Hu, B. Xiao, A. L. Tang, X. C. Wang and E. J. Zhou, *J. Mater. Chem. A*, 2018, **6**, 16769–16797; (*b*) G. D. Carlo, A. O. Birolib, F. Tessorea, S. Caramoric and M. Pizzotti, *Coord. Chem. Rev.*, 2018, **358**, 153–177; (*c*) M. A. Rajora, J. W. H. Lou and G. Zheng, *Chem. Soc. Rev.*, 2017, **46**, 6433–6469.

5 (*a*) Y. Ding, Y. Xie, X. Li, J. P. Hill, W. Zhang and W. Zhu, *Chem. Commun.*, 2011, **47**, 5431–5433; (*b*) Y. Ding, Y. Tang, W. Zhu and Y. Xie, *Chem. Soc. Rev.*, 2015, **44**, 1101–1112.

6 J. F. Wang, Y. H. Yao, Y. Y. Ning, Y. S. Meng, C. L. Hou, J. Zhang and J. L. Zhang, *Org. Chem. Front.*, 2018, **5**, 1877–1885.

7 R. Ziessel, P. Stachelek, A. Harriman, G. J. Hedley, T. Roland, A. Ruseckas and I. D. W. Samuel, *J. Phys. Chem. A*, 2018, **122**, 4437–4447.

8 B. Brocklehurst, *J. Phys. Chem.*, 1979, **83**, 536–543.

9 (*a*) A. Harriman, M. A. Alamiry, J. P. Hagon, D. Hablot and R. Ziessel, *Angew. Chem., Int. Ed.*, 2013, **52**, 6611–6615; (*b*) N. Hildebrandt, C. M. Spillmann, W. R. Algar, T. Pons, M. H. Stewart, E. Oh, K. Susumu, S. A. Diaz, J. B. Delehanty and I. L. Medintz, *Chem. Rev.*, 2017, **117**, 536–711; (*c*) K. D. Jordan and M. N. Paddonrow, *Chem. Rev.*, 1992, **92**, 395–410; (*d*) S. Speiser, *Chem. Rev.*, 1996, **96**, 1953–1976.

10 (*a*) J. W. Hong, H. Y. Woo, B. Liu and G. C. Bazan, *J. Am. Chem. Soc.*, 2005, **127**, 7435–7443; (*b*) S. W. Thomas, 3rd, G. D. Joly and T. M. Swager, *Chem. Rev.*, 2007, **107**, 1339–1386; (*c*) J. Fan, M. Hu, P. Zhan and X. Peng, *Chem. Soc. Rev.*, 2013, **42**, 29–43; (*d*) M. Y. Wong and E. Zysman-Colman, *Adv. Mater.*, 2017, **29**, 1605444; (*e*) S. K. Park, J. H. Kim and S. Y. Park, *Adv. Mater.*, 2018, **30**, 1704759.

11 (*a*) G. Bottari, G. de la Torre, D. M. Guldi and T. Torres, *Chem. Rev.*, 2010, **110**, 6768–6816; (*b*) S. Fukuzumi, K. Ohkubo and T. Suenobu, *Acc. Chem. Res.*, 2014, **47**, 1455–1464; (*c*) Z. M. Hudson, S. B. Ko, S. Yamaguchi and S. Wang, *Org. Lett.*, 2012, **14**, 5610–5613; (*d*) A. Shuto, T. Kushida, T. Fukushima, H. Kaji and S. Yamaguchi, *Org. Lett.*, 2013, **15**, 6234–6237; (*e*) R. P. Domingue and M. D. Fayer, *J. Phys. Chem.*, 1986, **90**, 5141–5146.

12 (*a*) L. Bucher, N. Desbois, P. D. Harvey, G. D. Sharma and C. P. Gros, *Sol. RRL*, 2017, **1**, 1700127; (*b*) Y. Ding, W. H. Zhu and Y. Xie, *Chem. Rev.*, 2017, **117**, 2203–2256.

13 (*a*) M. E. El-Khouly, J. B. Ryu, K. Y. Kay, O. Ito and S. Fukuzumi, *J. Phys. Chem. C*, 2009, **113**, 15444–15453; (*b*) C. G. Claessens, D. Gonzalez-Rodriguez and T. Torres, *Chem. Rev.*, 2002, **102**, 835–853.

14 Y. Gabe, Y. Urano, K. Kikuchi, H. Kojima and T. Nagano, *J. Am. Chem. Soc.*, 2004, **126**, 3357–3367.

15 E. V. De Wael, J. Pardoen, J. Van Koeveringe and J. Lugtenburg, *Recl. Trav. Chim. Pays-Bas*, 1977, **96**, 306–309.
16 L. Wang, K. Q. Zhu, Q. Chen and M. Y. He, *Dyes Pigm.*, 2015, **112**, 274–279.
17 A. Maity, A. Sarkar, A. Sil, B. N. S. Bhaktha and S. K. Patra, *New J. Chem.*, 2017, **41**, 2296–2308.
18 (*a*) G. L. Fu, H. Pan, Y. H. Zhao and C. H. Zhao, *Org. Biomol. Chem.*, 2011, **9**, 8141–8146; (*b*) L. Huang, X. Cui, B. Therrien and J. Zhao, *Chem. – Eur. J.*, 2013, **19**, 17472–17482; (*c*) L. Huang and J. Zhao, *RSC Adv.*, 2013, **3**, 23377–23388.
19 (*a*) M. Stepień and L. Latos-Grazyński, *J. Am. Chem. Soc.*, 2002, **124**, 3838–3839; (*b*) T. D. Lash, A. M. Young, J. M. Rasmussen and G. M. Ferrence, *J. Org. Chem.*, 2011, **76**, 5636–5651; (*c*) B. Szyszko, L. Latos-Grazynski and L. Szterenberg, *Chem. Commun.*, 2012, **48**, 5004–5006; (*d*) T. D. Lash, *Org. Biomol. Chem.*, 2015, **13**, 7846–7878.
20 Q. Zhou, M. Zhou, Y. Wei, X. Zhou, S. Liu, S. Zhang and B. Zhang, *Phys. Chem. Chem. Phys.*, 2017, **19**, 1516–1525.
21 (*a*) C. Lee, W. Yang and R. G. Parr, *Phys. Rev. B: Condens. Matter Mater. Phys.*, 1988, **37**, 785–789; (*b*) A. D. Becke, *J. Chem. Phys.*, 1993, **98**, 5648–5652; (*c*) P. C. Hariharan and J. A. Pople, *Theor. Chim. Acta*, 1973, **28**, 213–222; (*d*) M. M. Francl, W. J. Petro, W. J. Hehre, J. S. Binkley, M. S. Gordon, D. J. DeFree and J. A. Pople, *J. Chem. Phys.*, 1982, **77**, 3654–3665.
22 (*a*) C. B. Kc, G. N. Lim, V. N. Nesterov, P. A. Karr and F. D'Souza, *Chem. – Eur. J.*, 2014, **20**, 17100–17112; (*b*) S. S. Razi, Y. H. Koo, W. Kim, W. Yang, Z. Wang, H. Gobeze, F. D'Souza, J. Zhao and D. Kim, *Inorg. Chem.*, 2018, **57**, 4877–4890; (*c*) R. Ziessel, B. D. Allen, D. B. Rewinska and A. Harriman, *Chem. – Eur. J.*, 2009, **15**, 7382–7393.
23 (*a*) G. M. Sheldrick, *Acta Crystallogr., Sect. A: Found. Crystallogr.*, 2008, **64**, 112–122; (*b*) G. M. Sheldrick, *Acta Crystallogr., Sect. C: Struct. Chem.*, 2015, **71**, 3–8.
24 O. V. Dolomanov, L. J. Bourhis, R. J. Gildea, J. A. K. Howard and H. Puschmann, *J. Appl. Crystallogr.*, 2009, **42**, 339–341.
25 A. L. Spek, *Acta Crystallogr., Sect. D: Biol. Crystallogr.*, 2009, **65**, 148–155.
26 M. J. Frisch, G. W. Trucks, H. B. Schlegel, G. E. Scuseria, M. A. Robb, J. R. Cheeseman, G. Scalmani, V. Barone, G. A. Petersson, H. Nakatsuji, X. Li, M. Caricato, A. Marenich, J. Bloino, B. G. Janesko, R. Gomperts, B. Mennucci, H. P. Hratchian, J. V. Ortiz, A. F. Izmaylov, J. L. Sonnenberg, D. Williams-Young, F. L. F. Ding, J. G. F. Egidi, A. P. B. Peng, T. Henderson, D. Ranasinghe, V. G. Zakrzewski, N. R. J. Gao, G. Zheng, W. Liang, M. Hada, M. Ehara, K. Toyota, R. Fukuda, J. Hasegawa, M. Ishida, T. Nakajima, Y. Honda, O. Kitao, H. Nakai, T. Vreven, K. Throssell, J. J. A. Montgomery, J. E. Peralta, F. Ogliaro, M. Bearpark, J. J. Heyd, E. Brothers, K. N. Kudin, V. N. Staroverov, T. Keith, R. Kobayashi, J. Normand, K. Raghavachari, A. Rendell, J. C. Burant, S. S. Iyengar, M. C. J. Tomasi, J. M. Millam, M. Klene, C. Adamo, R. Cammi, J. W. Ochterski, R. L. Martin, K. Morokuma, O. Farkas, J. B. Foresman and D. J. Fox, *Gaussian 09, Revision D.01*, Gaussian, Inc., Wallingford CT, 2013.

